In vivo STED microscopy: a roadmap to nanoscale imaging in the living mouse

Heinz Steffens, Waja Wegner, Katrin Willig

Angaben zur Veröffentlichung / Publication details:

Steffens, Heinz, Waja Wegner, and Katrin Willig. 2020. "In vivo STED microscopy: a roadmap to nanoscale imaging in the living mouse." *Methods* 174: 42–48. https://doi.org/10.1016/j.ymeth.2019.05.020.

Methods 174 (2020) 42–48

Contents lists available at ScienceDirect

Methods

journal homepage: www.elsevier.com/locate/ymeth

In vivo STED microscopy: A roadmap to nanoscale imaging in the living mouse

Heinz Steffens[a,b], Waja Wegner[a,b], Katrin I. Willig[a,b,*]

[a] *Optical Nanoscopy in Neuroscience, Center for Nanoscale Microscopy and Molecular Physiology of the Brain, University Medical Center Göttingen, 37099 Göttingen, Germany*

[b] *Max Planck Institute of Experimental Medicine, Hermann-Rein-Str. 3, 37075 Göttingen, Germany*

ARTICLE INFO

Keywords:
Intravital
Superresolution
Nanoscopy
Cranial window
Dendritic spine

ABSTRACT

Superresolution microscopy techniques are now widely used, but their application in living animals remains a challenging task. The first superresolution imaging in a live vertebrate was demonstrated with STED microscopy in the visual cortex of an anaesthetized mouse. Here, we explain the requirements for a simple but robust *in vivo* STED microscope as well as the surgical preparation of the cranial window and the mounting of the mouse in detail. We have developed a mounting stage with a heating plate to keep the mouse body temperature stable and that can be adjusted to the optical axis of the microscope. We have optimised the design to avoid inducing thermal drift, which is critical for nanoscale imaging. STED microscopy with a resolution of 60 nm requires special cranial window preparation to avoid motion artefacts. We have implemented a drain tube to reduce the fluid between the glass window and the surface of the brain, which has been identified as the main cause for the motion artefacts. Together, these advances in the preparation allow the use of a simple intraperitoneal anaesthesia and make the previously used venous infusion and artificial respiration obsolete.

1. Introduction

In vivo fluorescence microscopy offers unique insights into the function of neurons in the intact nervous system by enabling studies of changes in cellular morphology in relation to experience or due to genetical or pathological modifications. Mouse models of neurological disease, for example, play an important role in elucidating disease processes and finding new therapies. A detailed assessment of activity dependent morphological changes in living animals, however, has so far been hampered by the diffraction-limit of light, whereas electron microscopy on the other hand allows only a static assessment. Hence, there is a huge potential to apply the nanoscopy (superresolution) methods [1], which enable sub-diffraction fluorescence microscopy, in living mice as well [2]. Nanoscopy methods include, among others, stimulated emission depletion (STED) microscopy [3], reversible saturable optical fluorescent transition microscopy (RESOLFT) [4], stochastic optical reconstruction microscopy (STORM) [5], and photoactivated localization microscopy (PALM) [6]. Of all these methods, STED microscopy is best suited for *in vivo* mouse imaging mainly due to its inherent 3D sectioning capability, which is ideal for tissue imaging, while using standard fluorescent proteins, such as the green or yellow fluorescent proteins (GFP, YFP) [2] or red-emitting fluorescent proteins [7]. Although, *in vivo* mouse STED microscopy was first demonstrated already in 2012 [2], only very few groups are working with this technique [8,9]. Here, we will discuss all steps towards *in vivo* mouse STED imaging of cortical structures in detail with focus on the window implantation and stable but adjustable mounting of the mouse. We describe a very basic but robust STED microscope setup which is attached to an upright microscope stand. The use of a microscope stand with a fluorescence unit and the use of visible fluorescence markers facilitates the first steps with *in vivo* STED microscopy, as the quality of the window, the distance of the brain surface to the cranial window, and the expression pattern as well as the brightness of the fluorescence labelling can be observed directly by eye. Importantly, nanoscale imaging requires high local stability of the imaging area in relation to the STED microscope. Any movement of the imaging area within the acquisition time caused by vibrations of the microscope, vital functions of the mouse such as heart beat, or pressure pulse, or thermal drift leads to distorted images. Moreover, we have developed an advanced mouse mounting stage with the potential of fine adjustment of the cranial window perpendicular to the optical beam path to reduce image distortions. Furthermore, we designed the mounting stage as a heat sink to

* Corresponding author at: Optical Nanoscopy in Neuroscience, Center for Nanoscale Microscopy and Molecular Physiology of the Brain, University Medical Center Göttingen, 37099 Göttingen, Germany.
E-mail address: kwillig@em.mpg.de (K.I. Willig).

https://doi.org/10.1016/j.ymeth.2019.05.020
Received 15 March 2019; Received in revised form 15 May 2019; Accepted 21 May 2019
Available online 24 May 2019

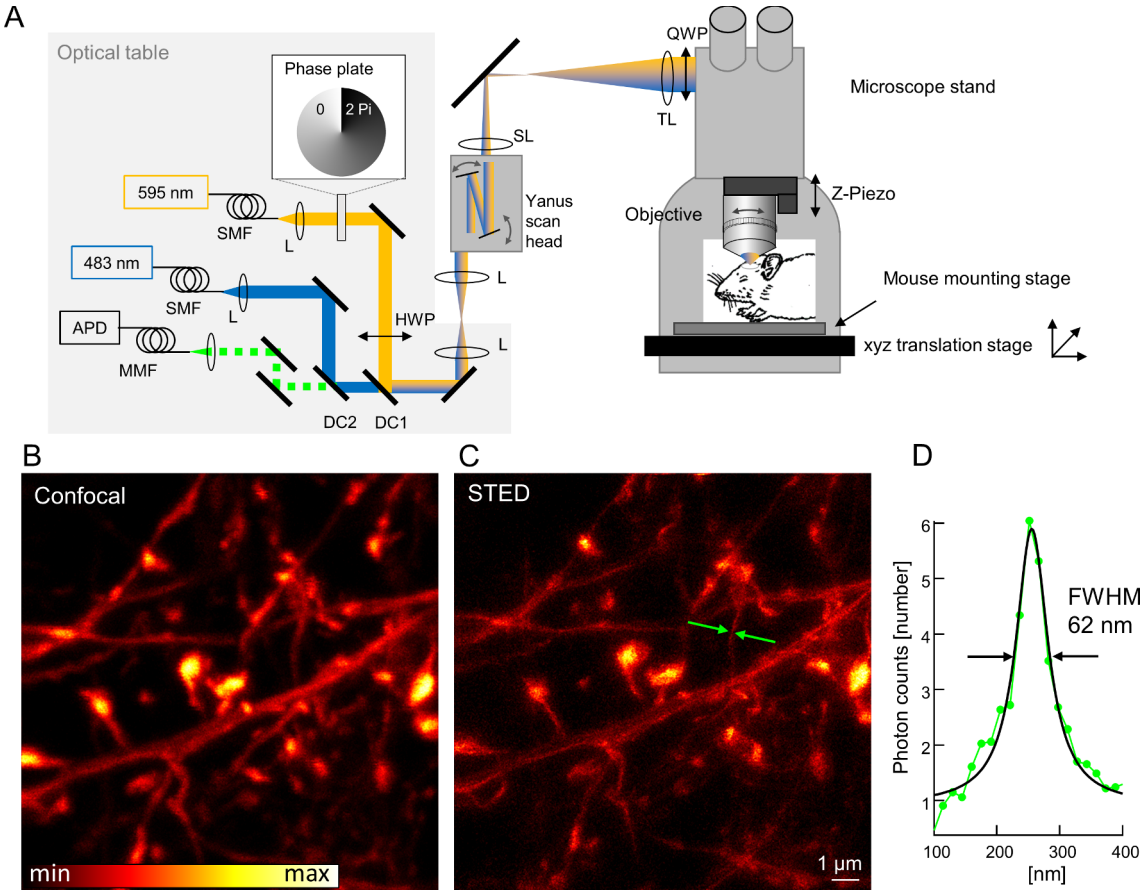

Fig. 1. Experimental layout of the *in vivo* STED microscopy technique. A Scheme of custom-made one-colour *in vivo* STED microscope. QWP: Quarter wave plate, HWP: Half wave plate, TL: Tube lens, SL: scan lens, L: lens, DC: Dichroic mirror, SMF: Single-mode fibre, MMF: Multi-mode fibre, APD: Avalanche photo diode detector. B, C The actin cytoskeleton is highlighted with Actin-Chromobody-Citrine and apical dendrites of layer 5 pyramidal visual cortex neurons are imaged in layer 1. STED microscopy (C) reveals the actin filaments in much more detail than confocal mode (B). D line profile of the marked filament in (C), average of 3 lines, Lorentz fit function shows that the filament is as small as 62 nm in full-width at half-maximum (FWHM).

avoid thermal drift. Critical is also the cranial window technique which allows for very short working distance of the objective lens.

2. STED microscopy on the cortex of anaesthetized mice

The following chapter outlines the microscope setup of a basic *in vivo* STED microscope. Due to the availability of transgenic animals, good photo stability and brightness, and ease of use, the simplest approach to *in vivo* imaging is to use EGFP, EYFP or related fluorescent protein markers. Moreover, fluorescent proteins can be easily genetically expressed e.g. using viral vector techniques [10], and lead to highly specific labelling without background in the surrounding cells. For a general and most flexible approach to *in vivo* STED microscopy, we therefore propose to use a STED microscope capable to image EGFP/EYFP [11]. Fig. 1A shows a STED microscope setup for one-colour *in vivo* imaging which focuses on a slim design without compromising the image quality or stability. A 483 nm excitation laser beam (PIL048X; A.L.S., Berlin, Germany) with ~70 ps long pulses is cleaned up spatially with a polarization-preserving single-mode fibre (PMJ, 3 m; OZ optics, Ottawa, Canada) for a single-mode beam profile and the collimated beam is merged with the STED beam by a short-pass dichroic mirror (DC1, HR640nm/HT UV; Laser Components, Olching, Germany). The epi-fluorescence signal is separated from the excitation light by a long-pass dichroic mirror (DC2, zt473rdcxt; Chroma Technology Corporation, Bellows Falls, VT), cleaned up by a band-pass filter (525/50; IDEX/Semrock, Rochester, NY) and detected by an avalanche photo diode (SPCM-AQRH-13, Excelitas Technologies, Waltham, MA) after passing a multi-mode fibre acting as confocal pinhole. The STED light is delivered by a Ti:Sapphire laser (MaiTai, Spectra-Physics, Darmstadt, Germany) pumped optical parametric oscillator (OPO; APE, Berlin, Germany) emitting 80 MHz pulses at 595 nm. The combination of a Ti:Sa with an OPO was chosen because of its tunability to adapt the STED wavelength for the use of fluorescent proteins with different spectral emissions. However, for the exclusive imaging of EGFP, EYFP or similarly emitting fluorescent proteins, this expensive combination can be replaced by now available 595 nm turn-key lasers. The pulses of the OPO are stretched to ~250 ps by dispersion in a glass rod (SF6, custom-made) and an 80 m long polarization-preserving optical fibre (PMJ; OZ Optics, Ottawa, Canada). The collimated STED beam passes a vortex phase plate (VPP-1b; RPC Photonics, Rochester, NY) and a half-wave plate (B. Halle Nachfl., Berlin, Germany). The vortex phase plate is imaged to the Yanus scan head (Till Photonics-FEI, Gräfelfing, Germany), which consists two galvanometric scanners and relay optics. The scan mirrors of the Yanus scan head are imaged with a scan and tube lens (Leica, Wetzlar, Germany) into the back pupil of the objective (PL APO, 63x, glycerol, 1.3NA; Leica, Wetzlar, Germany). The objective is equipped with a correction collar, which is used to compensate for spherical aberrations in the tissue [11]. Circular polarization of the STED beam is ensured by a quarter-wave plate (B. Halle Nachfl., Berlin, Germany) mounted directly before the beams enter the microscope stand (DM6000, Leica, Wetzlar, Germany). Z-stacks are recorded by piezo-scanning (MIPOS 100 PL CAP, piezosystem jena GmbH, Jena, Germany) the objective. The mouse, or any other sample, is coarsely aligned in x-y by a motorized translation stage (S-DM5000-FT; Applied

Scientific Instrumentation, Eugene, OR) which is mounted onto the microscope stand for z alignment. The microscope stand is equipped with a fluorescence unit, a camera (DMK72AUC02; The Imaging Source, Bremen, Germany), and a 4x objective for overview images. To ensure stability and convenience, we mounted, as far as possible, all parts of the STED microscope on the optical table, and then guided the light into the upright microscope stand after passing through the Yanus scan head. Special care needs to be taken for very rigid mounting of all parts above the optical table such as the scan head, the scan lens as well as the tube lens. For aberration-free imaging with water or glycerol immersion objectives, it is of outmost importance that the sample is well aligned perpendicular to the optical axis.

To demonstrate the *in vivo* image quality we labelled neuronal actin. Thus, we stereotaxically transduced layer 5 pyramidal neurons of an adult mouse by injection of adeno-associated viral particles (AAV) encoding for Actin-Chromobody-Citrine (Actin-Chromobody®; Chromotek, Planegg, Germany) into the visual cortex of the mouse [11,12]. Three weeks after transduction, we performed a craniotomy and imaged the visual cortex. Fig. 1B, C show several dendrites with dendritic spines attached. Actin is highly enriched in the spine head but forms thin filaments in the spine neck and dendritic arbor, which is resolved in much more detail with STED than in the confocal mode. It should be noted that actin labels must be expressed carefully since high expression levels can lead to morphological changes in neuronal cells such as the disappearance of dendritic spines [12]. While the STED microscope lined out here is very basic and well published, the key aspects for *in vivo* STED microscopy are the mouse mounting as well as the way the window is implanted after the craniotomy. Therefore, we will discuss the design of the mouse mounting stage and the surgical cranial window implantation procedure in detail in the next sections. For an overview see the quick start guide (Box 1).

Box1: Quick start guide

During the entire procedure, the depth of anaesthesia, body temperature and vital functions must be checked regularly!

1. *Anaesthetize mouse*
2. *Insert rectal temperature probe*
3. *Place mouse in stereotaxic frame*
4. *Apply gas inhalation*
5. *Apply ophthalmic ointment*
6. *Start monitoring vital functions*
7. *Remove scalp*
8. *Glue head bar to skull*
9. *Transfer mouse to custom-made mounting stage*
10. *Adjust/maintain mouse body temperature*
11. *Drill circular grove for craniotomy*
12. *Drill straight grove for drainage tube*
13. *Prepare drainage tube and fit into grove*
14. *Remove bone flap, dura and arachnoid mater*
15. *Cover craniotomy with prepared cover glass*
16. *Glue cover glass*
17. *If necessary: suck off excess fluid with syringe*
18. *Align cranial window perpendicular to optical axis*
19. *Transfer mouse to the microscope and image*

3. Mouse mounting stage

As a mounting stage we use a kinematic mount of an aluminium block (Fig. 2, (1)) resting on three steel spheres on a base plate (Fig. 2, (4)). One sphere is fixed, and resting on a cone at the lower left corner (Fig. 2, (p)). The other two spheres are on the tips of fine adjustment screws resting on grooves. These high-precision adjustment screws (Fig. 2, (f), Newport Corporation; Irvine, CA) allow fine adjustment of the specimen to be aligned parallel to the base plate and therefore perpendicular to the optical axis of the microscope. The aluminium block is fixed to the base plate by strong springs (Fig. 2, (s)). The head holder (Fig. 2, inset) is composed of a metal bar (Fig. 2, (b)) which is shaped to fit the curvature of the mouse skull. It is attached by a joint bearing (Fig. 2, (d)) to a 10 mm Ø stainless steel bar which is mounted by a cross connector to a rigidly fixed vertical steel bar (Fig. 2, (3)). Thus, the head holder can be coarsely adjusted relative to the 3 axes in space, i.e. height, tip and tilt.

Since anaesthetized mice loose central temperature control, they must be constantly warmed to stable ~36 °C. The insertion of a heating pad into a microscope setup is very critical, as indirect heating of the microscope parts leads to temporal expansion and thus induces thermal drift. The heat input also changes over time due to the continuous adjustments of the heating power due to temperature fluctuations of the mouse. To overcome these challenges, and after a few iterations, we integrated the heating as follows: A small heating pad (5 W, 24 V, 95 mm × 50 mm; Thermo technologies, Rohrbach, Germany) was implemented into the mounting stage and glued to the bottom surface of a stainless steel plate (Fig. 2, (2)). During each experiment, the heating pad is covered with a diathermic sterile fabric underlay and the body temperature of the mouse is monitored by inserting a rectal temperature sensor. The heat plate is as small as possible but is still under the complete adult mouse. It sits in a recess within the aluminium block (Fig. 2, (1)) with a 5 mm distance to the walls of the recess. The bottom of the heat plate is thermally insulated from the aluminium block by a 2 mm cork layer and is fixed against shifting by 4 thin steel pins fitting into 4 holes in the aluminium block. The relatively large aluminium block acts as a heat buffer; its large size compared to the heat plate and its thermal insulation prevent significant heating of the aluminium block. Thus, necessary corrections of the mouse body temperature do not lead to significant temperature shifts of the aluminium block. Mounting the aluminium block on three spheres additionally reduces the heat flow from the aluminium block to the base plate and prevents further heating of the microscope. The temperature of the heating pad needs to be slightly adapted over the entire measurement time to keep the temperature of the mouse constant. We decided to perform the temperature control manually, which is simpler than closed loop temperature control. Manual control provides attentiveness to temperature changes and thus information about the vital state of the mouse. We perform installation of the cranial window on the mounting stage, which gives the mounting stage enough time to reach a thermally stable state.

Our custom-made mouse mounting stage weights 2.0 kg and is therefore relatively heavy. Hence, a microscope stage that is able to carry this weight without causing damage or drift is required.

4. Anaesthesia and monitoring

In our previously published work, we preferred to control anaesthesia by permanent venous infusion and artificial respiration after tracheotomy [2,11,12,13]. This procedure was quite time consuming, but had the main advantage of flat respiration with a gas mixture with high O_2 (47.5 vol%) content and the possibility of using a muscle relaxant to avoid active movement of the respiratory skeletal muscles. Thus, respiratory artefacts during imaging could be eliminated.

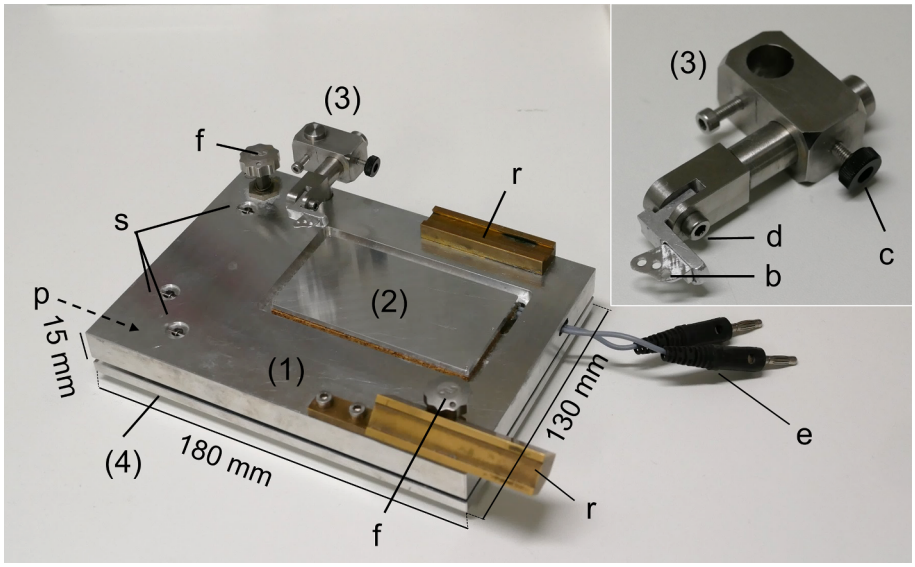

Fig. 2. Mouse mounting stage with the main aluminium block (1), the heat plate (2), the head holder (3), and the base plate (4). Inset shows a magnified view of the head holder (3) with the head bar (b). Coarse adjustment of the mouse head is performed by rotating (c) or tilting (d) the head holder. Two fine adjustment screws (f) are used to tilt the main block (1) around the pivot point (position (p), not visible). The main block is held to the 5 mm aluminium base plate by strong springs (*s*). (e) Connectors for the heat pad underneath the heat plate; fixed rails (*r*) to mount additional tools if necessary.

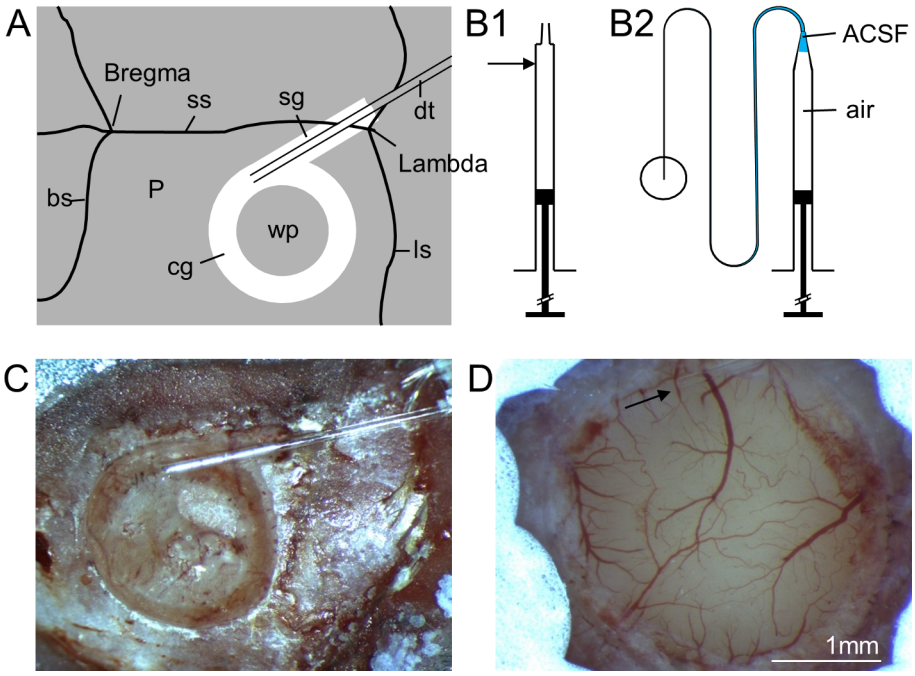

Fig. 3. Outline of the craniotomy. A Surface of the skull with circular groove (cg) and straight groove (sg) drilled. The drain tube (dt) is fixed to the straight groove. Grooves are ~0.7 mm wide, according to the drill size. bs bregmoid suture; ls lambdoid suture; ss sagittal suture; P parietal bone (left); wp window plate. B The drain tube is made from a 1 ml polypropylene syringe, which was heated and elongated. B1 apply heat at position of the arrow. B2 Extended PP syringe. The tube is filled with ACSF (blue). Note the large air volume in the syringe. The encircled end of the tube is glued to the straight groove (A, sg). C Example preparation image with 2 mm Ø circular groove. D View of the brain surface after finishing the window preparation; note the drain tube (arrow). (For interpretation of the references to colour in this figure legend, the reader is referred to the web version of this article.)

However, motion artefacts by the pressure pulse (heart beat) remained. In the meantime, we have refined our cranial window preparation and fixation of the head bar, which resulted in a stabilization of the whole preparation. Our initial problem of motion artefacts due to vital functions was thereby solved, which made the tracheotomy unnecessary. Now, we are using a much simpler intraperitoneal anaesthesia with Fentanyl (0.05 mg/kg), Midazolam (5 mg/kg), and Medetomidin (0.5 mg/kg). Throughout the whole experiment, we monitor vital functions such as O_2 saturation and pulse rate with a pulse oximeter located at the mouse thigh (MouseOX, Starr Life Sciences, Oakmont, PA) and the temperature with a rectal temperature probe. During anaesthesia we apply a gas mixture with high O_2 (47.5 vol%) and CO_2 (2.5 vol%) content over a cone in front of the mouse nose to be able to hold the O_2 saturation of the blood close to 98% and to keep the breath rate simultaneously on a low level.

5. Cranial window preparation for STED microscopy

The basis for the preparation of the cranial window is a tightly fixed head. At the beginning of the cranial window preparation, we use a stereotaxic frame (Narishige, Tokyo, Japan) to fix the mouse head in order to glue the metal head bar to the skull. We remove the scalp from the skull as necessary and clean it from connective tissue by a micro curette (10082-15; Fine Science Tools GmbH, Heidelberg, Germany) or the drill we need later for the craniotomy. The wound edges of the remaining skin are closed with the tissue adhesive n-Butyl cyanoacrylate (Histoacryl®, B. Braun Melsungen AG, Melsungen, Germany). The head bar (Fig. 2, (b)) is then glued to the skull with dental adhesive resin cement, a cement with polymethyl methacrylate being the main component (Super-Bond C&B, Sun Medical Co. LTD, Japan) [9]. When gluing the holder to the skull it is important to leave enough space for the bulky high numerical aperture objective lens used for STED microscopy. After hardening of the dental cement, the mouse is moved to the mounting stage (Fig. 2) and the head bar is fixed to the head holder

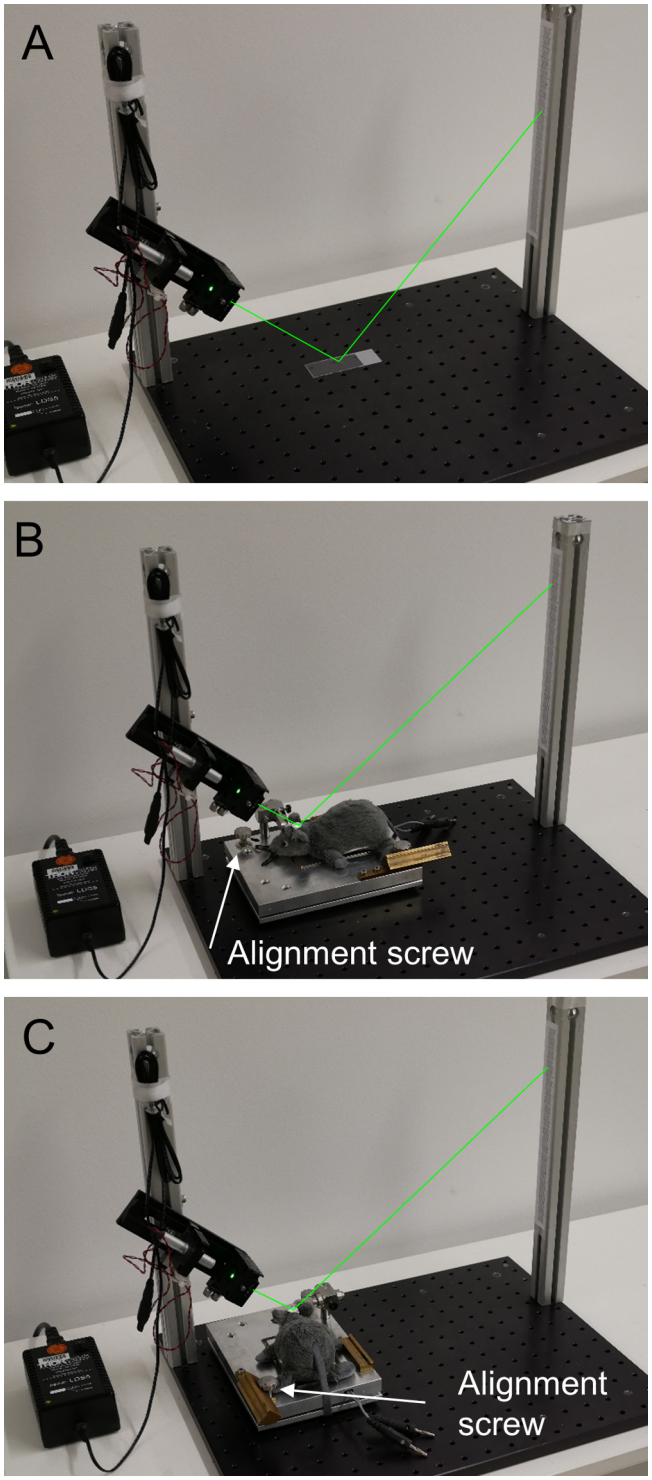

Fig. 4. Optical alignment device. A The green laser beam of a 532 nm laser diode is reflected by a microscope slide which lays parallel to the mounting plate onto a vertically aligned scale bar to define the centred position of the beam. B, C Depiction of mouse alignment. Tilt of the cover glass on the cranial window results in off-centre projection. The fine screws are used to align the projection for one axis after the other to the before defined centred position (A) on the scale. As the cranial window is at a higher level (with respect to the z-axis) as the microscope slide, which was used for the initial alignment, the reflection of the laser beam hits the scale (vertical device covered with millimetre paper) at a higher position (B, C). The marked screws in B, C are used to align the cover glass perpendicular to the plane of the STED laser beam. (For interpretation of the references to colour in this figure legend, the reader is referred to the web version of this article.)

(Fig. 2, inset). In a next step, a circular groove (~2.5 mm Ø) is drilled (Drill: 216804; RUDOLF FLUME Technik GmbH, Essen, Germany; drilling head: HP 310 104 001 001 007; Hager & Meisinger GmbH, Neuss, Germany) at the designated region of interest, e.g. above the visual cortex (Fig. 3A). Drilling is performed until the bottom of the groove is flexible, but without impairing the brain surface. Care has to be taken during this process not to damage the underlying brain tissue either by heating up the bone or piercing through the skull. The drill has to be moved permanently because drilling the same one location for more than 1 s leads to overheating. A second straight groove ending tangentially at the circular groove is drilled to take up a thin drain tube (Fig. 3A). The drain tube is made by heating and extending a 1 ml polypropylene syringe (BD Plastipak™, Becton Dickinson S.A., Madrid, Spain) (Fig. 4B). The tube can be extended to ~0.2 mm Ø (Fig. 3B). The extended tube is back-filled with artificial cerebrospinal fluid (ACSF), just to the tip of the remaining syringe, so that a large air reservoir (> 0.5 ml) is created after backfilling the tube. The end of the tube is glued to the straight groove so that its tip ends in the circular groove (Fig. 3A). It has to be thin enough to fit into the groove and not protrude the skull surface. The encircled window bone plate can be removed after wetting the circle groove and the window bone plate (Fig. 3C). Together with the bone plate, the dura mater comes off (possibly only the outer layer of the dura mater). Thin pieces of bone may also remain on the brain surface, which have to be removed carefully by using either forceps or washing the area with ACSF. The brain surface is still covered with a thin layer of meninges, of which the remainders of the dura and arachnoid mater have to be removed with a biology type fine forceps (No. 5 Biology tip, Fine Science Tools) to improve the STED image quality. It is particularly important to ensure that the surface of the brain stays always wet and is not injured during this procedure. After flushing the surface several times with ACSF to remove eventually resting blood cells or other disturbing free particles, the cover glass (6 mm Ø, #1.5; Paul Marienfeld GmbH & Co. KG, Lauda-Königshofen, Germany) is glued above the hole in the bone. In a first step we use Histoacryl®, which preferentially closes wet surfaces without mixing up with the fluid under the cover glass. The procedure to glue the round cover glass to the bone, together with the drain tube underneath is quite delicate. Therefore, we put a tiny custom-made cylindrical brass weight (~0.7 g) on the cover glass to hold it down during gluing with Histoacryl®. Histoacryl® is applied with a fine pipette tip (GELoader 0030 001.222; Eppendorf AG, Hamburg, Germany) to reach under the edge of the cover glass. To be able to estimate the distance between the cover glass and the brain surface during microscopy, we add a thin layer of fluorescent beads (FluoSpheres™, yellow-green, 40 nm; Thermofisher, Waltham, MA) on the poly-L-lysine (P4707; Sigma-Aldrich, Taufkirchen, Germany) coated lower surface of the cover glass. Another advantage of using fluorescent beads is that the STED microscope alignment and quality of the immersion fluid can be controlled by imaging these fluorescent beads anytime during the imaging experiment. A thin layer of silicon polymer (First Contact; Photonic Cleaning Technologies, Platteville, WI) applied to the middle of the cover glass will protect the glass surface from dirt and scratches until the end of the cranial window procedure. The final fixation of the cover glass to the skull is performed by using dental cement (Super-Bond C&B, Sun Medical Co. LTD, Japan). Therefore we apply the cement around the cover glass to form a solid cement block which connects the skull, head bar, and cover glass firmly with each other. Again, care has to be taken that there remains enough space for the bulky objective lens of the microscope. It turned out that Super-Bond improved the quality and stability of our window preparation significantly [9]. For example, the dental cements we had used before induced a curvature on the cover glass which was probably due to a shrinkage of the cement after curing. In addition, we often observed drift with other dental cements probably due to the longer curing time and the persistent shrinkage of the cement over the imaging period. After the Super-Bond has cured, the protective silicon polymer can be removed from the

cover glass surface and any excess fluid can be sucked off using the syringe and drain tube if required (Fig. 3D). It is very important that a large volume of air remains in the syringe to avoid excessive negative pressure when sucking excess fluid from the chamber under the cover glass. Pulling has to be done gently, since too much suction reduces the blood perfusion of the cortex and leads to neuronal death. However, a small fluid ring should remain on the outer part of the window, while the middle part of the visible brain surface should be attached to the glass. The distance between the cover glass (fluorescent beads) and brain structures is typically about 3–5 μm. Under these conditions, STED microscopy is possible without disturbing movements caused by respiration or blood pressure pulses. It is self-evident, that near arteries (there will always be two or three of them in the window field), pressure pulse artefacts cannot be avoided.

6. Mouse (cranial window) alignment procedure

Prior to imaging, the cranial window has to be aligned perpendicularly to the optical axis of the microscope to improve the image quality. The microscope is aligned so that the optical axis is perpendicular to the x-y translation stage (Fig. 1) and therefore also perpendicular to the mouse mounting base plate (Fig. 2, (4)), which is attached to the x-y translation stage. First, we tried an “on-stage” alignment by tilting the mounting stage with the fine screws until the cover glass on the cranial window was parallel to the focal plane. In order to be able to make a statement about the alignment of the cover glass, we coated its bottom surface with fluorescent beads, which could be visualized with the fluorescence widefield implemented in the STED microscope. However, this procedure turned out to be quite inconvenient as the tip and tilt of the stage introduces a major shift of the window up or down. Therefore, this method proved to be very time consuming, especially due to the short working distance of our high numerical aperture objective.

Consequently, we developed a simple system to adjust the cranial window “off-stage”. We mounted a low power green laser diode (CPS532, 4.5 mW, Thorlabs, Newton, NJ) on an optical breadboard (Fig. 4) which is aligned so that the beam is reflected on a flat, horizontal microscope slide to a vertical device opposite to the laser source, for example covered with millimetre paper (Fig. 4, A). Similar to the microscope slide the implanted cranial window reflects enough laser light and the reflection can therefore be used to align the glass window parallel to the mounting plate. Independent of the height of the reflecting glass surface, the cover glass is parallel to the plane of the breadboard, if the spot of the reflected beam stays constantly at its location when the holder with the mouse is rotated horizontally by 90° (Fig. 4, C). In other words, the cover glass is exactly perpendicularly aligned to the laser beam of the microscope. Rough alignment can be achieved by the adjustment of tip and tilt at the head holder (Fig. 2, (b, d)) and fine tuning is performed by the two high-precision adjustment screws (Fig. 2, (f)). The advantage of the “off-stage” adjustment is obvious, because it is done at a comfortable space for the adjustment of the mounting stage within < 2 min.

7. Summary and outlook

We have outlined a detailed description of our improved technique on how to set up cranial window preparation and mouse alignment to successfully perform superresolution *in vivo* STED imaging in the cortex of an anaesthetized mouse. To this end, we have developed a mouse mounting stage that includes a heating plate that is thermally isolated from the rest of the stage and thus does not cause thermal drift, and that can be used to regulate the mouse body temperature throughout the experiment. In addition, this stage is designed to be fine adjustable, allowing the cranial window to be aligned perpendicular to the optical beam path to avoid image distortion. The head of the mouse is mounted by a special designed head holder which is glued to the mouse skull. The cranial window technique has been significantly refined by the implantation of a drain tube that allows excess brain fluid to be carefully sucked off, reducing the distance between the brain surface and the cover glass, thereby substantially reducing motion artefacts. A further improvement of the cranial window procedure was the use of the new adhesive which does not induce a curvature on the cover even after an imaging time of up to 6 h. Taken together, these advances in stable preparation allow us the use of simple intraperitoneal anaesthesia instead of the previously used venous infusion of the anaesthetic and artificial respiration. These refinements paved the road to long term imaging such as chronic *in vivo* STED imaging. We have designed the head bar small enough to remain on the awake animal and will test now the capability and robustness to perform chronic *in vivo* STED imaging. This would give us the possibility to image morphological changes over a time period of days to month and to include e.g. paradigms to study learning and memory.

8. Hints for troubleshooting

- Head bar cannot be fixed properly on the skull: Before gluing the head bar with dental cement make sure the skull is roughened and dry. Wait long enough for the cement to harden, this can take up to 10–15 min.
- Bleeding after bone plate removal: Sometimes a bleeding cannot be avoided and should be washed excessively. Therefore, wash the craniotomy several times with ACSF to remove any blood cells. In case a virus was injected before, avoid removing the bone and dura at the injection site. Removing fused tissue caused by wound healing most likely causes damage and bleeding.
- Histoacryl® gets under the cover glass while fixing it and damages brain surface: Make sure that the cover glass is sufficiently weighted so that it rests directly on the skull bone. Fluid under the cover glass should reach to the edge of the cover glass in a way that the applied Histoacryl® encloses enough fluid while fixing and sealing the cover glass reliably.
- Motion artefacts: (1) If the surface brain structures move with the pressure pulse, and the fluorescent beads on the bottom of the cover glass do not, there is most likely too much fluid (distance) between the brain surface and the glass, i.e. the brain is not attached to the glass. Pull gently on the drain tube. (2) If the brain structures are drifting slowly and/ or the fluorescent beads on cover glass show motion artefacts, the head bar or the cover glass are not properly attached. The distance between surface neuronal structures and cover glass should be < 5 μm.
- Pulling the drain tube shows no effect: (1) After pulling, the plunger is slowly moving back to the original position: The tip of the tube is most likely blocked by tissue or dental cement. (2) Fluid cannot be removed although the plunger has moved a lot. Either leaky drain tube outside the chamber of the brain or leaky chamber. In both cases terminate experiment if image quality is not good enough.
- Brain structures are moving out of focus when moving the mouse in x-y: The objective, in STED microscopy typically one with a short working distance of $\sim$200–300 μm, is most likely touching the head of the mouse either at the head bar or at a small elevation of the cement. Remove excess cement with drill and level cranial window again before imaging.
- Vital functions of the mouse decrease slowly but steadily after some time of imaging: Check the position of the pulse oximeter and change its position (leg) as well as the positioning of the oxygen supply if necessary.

Acknowledgement

We thank S.W. Hell for support of the initial experiments and the precision mechanics workshops of the MPI for Biophysical Chemistry and MPI of Experimental Medicine for excellent work on the mouse

mounting stage. We are grateful to S. Liebscher, LMU Munich, for proposing the use of the intraperitoneal anaesthesia and J. Jethwa for proof reading. This work was supported by grants of the Deutsche Forschungsgemeinschaft through the DFG Research Center “Nanoscale Microscopy and Molecular Physiology of the Brain” and Cluster of Excellence EXC171 (Area A1).

All mouse experiments were performed according to the guidelines of the national law (Tierschutzgesetz der Bundesrepublik Deutschland, TierSchG) regarding animal protection procedures and approved by the responsible authorities, the Niedersächsisches Landesamt für Verbraucherschutz und Lebensmittelsicherheit (LAVES, Oldenburg, Germany).

References

[1] C. Eggeling, K.I. Willig, S.J. Sahl, S.W. Hell, Lens-based fluorescence nanoscopy, Q. Rev. Biophys. 48 (2015) 178–243, https://doi.org/10.1017/s0033583514000146.

[2] S. Berning, K.I. Willig, H. Steffens, P. Dibaj, S.W. Hell, Nanoscopy in a living mouse brain, Science 335 (2012) 551–552, https://doi.org/10.1126/science.1215369.

[3] S.W. Hell, J. Wichmann, Breaking the diffraction resolution limit by stimulated emission: stimulated-emission-depletion fluorescence microscopy, Opt. Lett. 19 (1994) 780, https://doi.org/10.1364/OL.19.000780.

[4] T. Grotjohann, I. Testa, M. Leutenegger, H. Bock, N.T. Urban, F. Lavoie-Cardinal, K.I. Willig, C. Eggeling, S. Jakobs, S.W. Hell, Diffraction-unlimited all-optical imaging and writing with a photochromic GFP, Nature 478 (2011) 204–208, https://doi.org/10.1038/nature10497.

[5] M.J. Rust, M. Bates, X. Zhuang, Sub-diffraction-limit imaging by stochastic optical reconstruction microscopy (STORM), Nat. Methods. 3 (2006) 793–796, https://doi.org/10.1038/nmeth929.

[6] E. Betzig, G.H. Patterson, R. Sougrat, O.W. Lindwasser, S. Olenych, J.S. Bonifacino, M.W. Davidson, J. Lippincott-Schwartz, H.F. Hess, Imaging intracellular fluorescent proteins at nanometer resolution, Science 313 (2006) 1642–1645, https://doi.org/10.1126/science.1127344.

[7] A. Miyawaki, D.M. Shcherbakova, V.V. Verkhusha, Red fluorescent proteins: Chromophore formation and cellular applications, Curr. Opin. Struct. Biol. 22 (2012) 679–688, https://doi.org/10.1016/j.sbi.2012.09.002.

[8] T. Pfeiffer, S. Poll, S. Bancelin, J. Angibaud, V.K. Inavalli, K. Keppler, M. Mittag, M. Fuhrmann, U.V. Nägerl, Chronic 2P-STED imaging reveals high turnover of dendritic spines in the hippocampus in vivo, Elife 7 (2018) 1–17, https://doi.org/10.7554/eLife. 34700.

[9] J.-M. Masch, H. Steffens, J. Fischer, J. Engelhardt, J. Hubrich, J. Keller-Findeisen, E. D’Este, N.T. Urban, S.G.N. Grant, S.J. Sahl, D. Kamin, S.W. Hell, Robust nanoscopy of a synaptic protein in living mice by organic-fluorophore labeling, Proc. Natl. Acad. Sci. 115 (2018) E8047–E8056, https://doi.org/10.1073/pnas.1807104115.

[10] T.B. Lentz, S.J. Gray, R.J. Samulski, Viral vectors for gene delivery to the central nervous system, Neurobiol. Dis. 48 (2012) 179–188, https://doi.org/10.1016/j.nbd.2011.09.014.

[11] K.I. Willig, H. Steffens, C. Gregor, A. Herholt, M.J. Rossner, S.W. Hell, Nanoscopy of filamentous actin in cortical dendrites of a living mouse, Biophys. J. 106 (2014), https://doi.org/10.1016/j.bpj.2013.11.1119.

[12] W. Wegner, P. Ilgen, C. Gregor, J. van Dort, A.C. Mott, H. Steffens, K.I. Willig, In vivo mouse and live cell STED microscopy of neuronal actin plasticity using far-red emitting fluorescent proteins, Sci. Rep. 7 (2017) 11781, https://doi.org/10.1038/s41598-017-11827-4.

[13] H. Steffens, F. Nadrigny, F. Kirchhoff, Preparation of the mouse spinal column for single imaging using two-photon laser-scanning microscopy, Cold Spring Harb. Protoc. 2012 (2012) 1280–1285, https://doi.org/10.1101/pdb.prot072249.